

Electron Delocalization in Mixed-Valence Keggin Polyoxometalates. Ab Initio Calculation of the Local Effective Transfer Integrals and Its Consequences on the Spin Coupling

Nicolas Suaud,* Alejandro Gaita-Ariño, Juan Modesto Clemente-Juan, José Sánchez-Marín, and Eugenio Coronado*

Contribution from the Instituto de Ciencia Molecular, Universidad de Valencia, C/Doctor Moliner 50, 46100 Burjassot, Spain

Received July 22, 2002

Abstract: We present a quantitative evaluation of the influence of the electron transfer on the magnetic properties of mixed-valence polyoxometalates reduced by two electrons. For that purpose, we extract from valence-spectroscopy ab initio calculations on embedded fragments the value of the transfer integrals between W nearest-neighbor atoms in a mixed-valence $\alpha\text{PW}_{12}\text{O}_{40}$ polyoxowolframate Keggin anion. In contradiction with what is usually assumed, we show that the electron transfer between edge-sharing and corner-sharing WO_6 octahedra have very close values. Considering fragments of various ranges, we analyze the accuracy of calculations on fragments based on only two WO_5 pyramids which should allow a low cost general study of transfer parameters in polyoxometalates. Finally, these parameters are introduced in an extended Hubbard Hamiltonian that models the whole anion. It permits to prove that electron transfers induce a large energy gap between the singlet ground state and the lowest triplet states providing a clear explanation of the diamagnetic properties of the mixed-valence Keggin ions reduced by two electrons.

I. Introduction

Polyoxometalates (POM) are a class of inorganic compounds with a remarkable degree of molecular and electronic tunabilities that impact disciplines as diverse as catalysis,¹ medicine,² and materials science.³ These compounds are molecular metal oxides mainly based on V, Mo, and W ions in their highest oxidation states. Because of the cluster structure, POM are specially useful as model systems for the studies of magnetic and electronic interactions. Indeed, many of these structures allow the inclusion of well-isolated clusters of paramagnetic ions with various nuclearities and definite topologies and geometries.⁴ On the other hand, they permit the controlled injection of electrons, giving rise to mixed-valence species in which delocalized electrons may coexist and interact with localized magnetic moments. In this context, they provide unique systems for the development of new theories in the mixed valence area.

Some typical structural types are the Lindquist⁵ ($\text{M}_6\text{O}_{19}^{2-}$, M = Mo, W), Keggin⁶ ($\text{XM}_{12}\text{O}_{40}^{m-}$, X = P, Si, Co, Ni, ...),

and Dawson–Wells⁷ ($\text{P}_2\text{M}_{18}\text{O}_{62}^{n-}$). The Keggin structure is constituted of four edge-sharing triads of MO_6 octahedra arranged around the X atom in such a way that the resulting species has a tetrahedral symmetry. The Keggin structure can also be viewed as formed by a XO_4^{m-} clathrate encapsulated into a neutral $\text{M}_{12}\text{O}_{36}$ sphere based on corner sharing MO_5 square–pyramids whose apical oxygen atoms point outside the sphere^{8,9} (see Figure 1a). They are thus sometimes noted as $\text{XO}_4^{m-} \subset \text{M}_{12}\text{O}_{36}$.

An important property of the polyoxometalate anions is that their identity is usually preserved by reversible redox processes,¹⁰ forming “heteropoly blues” or “heteropoly browns” reduction products by addition of various electrons which are delocalized over the sphere.¹¹ Experimentally, it has been found that when the reduced species contain an even number of delocalized electrons, their spins are always completely paired, even at room temperature. This result is general and has been found not only in the Keggin structure but also in the other

- * E-mail: Nicolas.Suaud@uv.es, Eugenio.Coronado@uv.es
- (1) Kozhevnikov, I. V. *Chem. Rev.* **1998**, *98*, 171. Mizuno, N.; Misono, M. *Chem. Rev.* **1998**, *98*, 199. Sadakane, M.; Steckhan, E. *Chem. Rev.* **1998**, *98*, 219.
 - (2) Rhule, J. T.; Hill, C. L.; Judd, D. A.; Schinazi, R. F. *Chem. Rev.* **1998**, *98*, 327.
 - (3) Müller, A.; Peters, F.; Pope, M. T.; Gatteschi, D. *Chem. Rev.* **1998**, *98*, 239. Coronado, E.; Gómez-García, C. J. *Chem. Rev.* **1998**, *98*, 273. Klemperer, W. G.; Wall, C. G. *Chem. Rev.* **1998**, *98*, 297. Pope, M. T.; Müller, A. *Polyoxometalates: From Platonic Solids to Anti-Retroviral Activity*; Kluwer Academic Publishers: Dordrecht, The Netherlands, 1994.
 - (4) Clemente-Juan, J. M.; Coronado, E. *Coord. Chem. Rev.* **1999**, *193*–195, 361.
 - (5) Lindquist, I. *Ark. Kemi* **1952**, *5*, 247.

- (6) Keggin, J. F. *Nature* **1933**, *131*, 908.
- (7) Dawson, B. *Acta Crystallogr.* **1953**, *6*, 113.
- (8) Brown, G. M.; Noe-Spirlet, M.-R.; Busing W. R.; Levy, H. A. *Acta Crystallogr.* **1977**, *B33*, 1038.
- (9) Rocchiccioli-Deltcheff, C.; Thouvenot, R.; Franck, R. *Spectrochim. Acta* **1976**, *5A32*, 87. Acerete, R.; Casañ-Pastor, N.; Bas-Serra, J.; Baker, L. C. W. *J. Am. Chem. Soc.* **1989**, *111*, 6049. Kazansky, L. P.; McGarvey, B. R. *Coord. Chem. Rev.* **1999**, *188*, 157. Maestre, J. M.; Lopez, X.; Bo, C.; Poblet, J.-M.; Casañ-Pastor, N. *J. Am. Chem. Soc.* **2001**, *123*, 3749. López, X.; Maestre, J. M.; Bo C.; Poblet, J.-M. *J. Am. Chem. Soc.* **2001**, *123*, 9571.
- (10) Casañ-Pastor, N.; Gómez-Romero, P.; Jameson, G. B.; Baker, L. C. W. *J. Am. Chem. Soc.* **1991**, *113*, 5658.
- (11) Pope, M. T. *Isopoly and Heteropoly Metalates*; Springer-Verlag: Berlin, 1983. Müller, A.; Krickemeyer, E.; Penk, M.; Wittneben, V.; Döring, J. *Angew. Chem., Int. Ed. Engl.* **1990**, *32*, 1780.

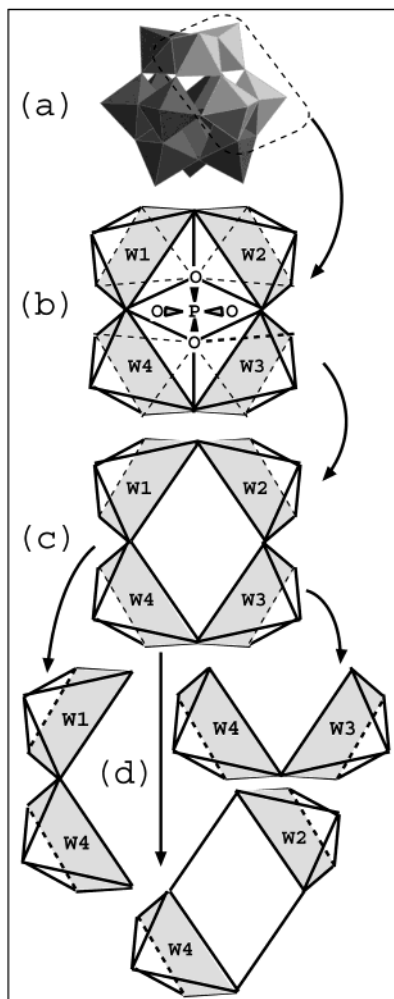


Figure 1. (a) Schematic structure of a Keggin anion. (b) The PW_4O_{20} fragment. (c) The W_4O_{16} fragment. (d) The three 2W-based fragments. The oxygen atoms occupy the corners of the octahedra or pyramids. The atoms modeled by punctual charges and TIPs are not represented.

ones. It was initially attributed to a very strong antiferromagnetic coupling via a multiroute superexchange mechanism,¹² but more recently, it has been theoretically shown that a combination of electron repulsion and electron delocalization can also stabilize the singlet ground state.^{13–15}

The extended-Hubbard model Hamiltonian used for these calculations handles the effective parameters corresponding to the main microscopic interactions: (i) the t electron transfer (hopping) parameter between corner-sharing MO_6 octahedra, (ii) the t' electron transfer (hopping) parameter between edge-sharing octahedra, (iii) the U on-site electron repulsion between electrons belonging to the magnetic orbital of a same metal center, (iv) the five $V_1 \dots V_5$ intersite electron repulsions corresponding to the five inequivalent pairs of metal centers.

Using this model, it may be possible to qualitatively explain the strong antiferromagnetic coupling between the pair of electrons in the reduced Keggin anion. However, the space spanned by this number of parameters is by far too large to permit an univoque solution of the problem. To reduce the size of this space and thus to draw a picture of the coupling between the two delocalized electrons, independent information on the values of these parameters is essential. The main aim of the present article is to evaluate theoretically some of these parameters. To reach this goal, we will calculate the transfer parameters t and t' by using very accurate ab initio methods. These values will be then introduced in the extended Hubbard model in order to obtain information on the lowest lying spin levels of the system and on the effective coupling between the pair of electrons that are delocalized over the Keggin structure.

II. Embedded Fragments

The transfer (hopping) effective integrals are essentially local parameters.¹⁶ Therefore, fragment spectroscopy calculations can be used to accurately evaluate their values. The fragments are embedded in a bath adapted to reproduce the main effects of the rest of the crystal, namely, the short-range Pauli exclusion and the long-range Madelung potential. This bath consists of a large number of punctual charges and total-ion pseudopotentials¹⁷ (TIPs). A quasi-spherical embedding of punctual charges is obtained by replacing all the atoms surrounding the fragment (those closer than 20 Å from the center of the considered Keggin anion) by punctual charges. The total-ion pseudopotentials, TIPs, are put in the position of all the atoms of the first and second shells enclosing the fragment. In refs 18 and 19, a complete description of embedded fragment spectroscopy calculations is reported as well as a discussion of the accuracy of the embedding procedure.

The biggest fragment of the Keggin cluster on which we have performed calculations is represented by the PW_4O_{20} tetramer (Figure 1b). This fragment is based on four adjacent WO_6 octahedra and on the PO_4 encapsulated clathrate. W1 and W2 belong to the same triad (and thus belong to edge-sharing WO_6 octahedra); W3 and W4 are part of the same triad (and thus belong to edge-sharing WO_6 octahedra) adjacent to the triad of W1 and W2. W1 and W4, on one side, and W2 and W3, on the other side, belong to corner-sharing octahedra. Such a fragment thus permits the electron delocalization along corner-sharing octahedra (t parameter), along edge-sharing octahedra (t' parameter), and between second neighbors octahedra (t'' parameter).

Figure 1c represents the W_4O_{16} fragment, extracted from the precedent PW_4O_{20} fragment by substituting the PO_4 molecule by the appropriated punctual charges and TIPs. It is thus composed of four corner-sharing WO_5 pyramids. A comparison between the values of the transfer parameters obtained on the PW_4O_{20} and W_4O_{16} fragments permits evaluation of the role that the PO_4 plays on the electron delocalization. This is so because punctual charges and TIPs do not support any basis

- (12) Kozik, M.; Hammer, C. F.; Baker, L. C. W. *J. Am. Chem. Soc.* **1986**, *108*, 2748. Kozik, M.; Baker, L. C. W. *J. Am. Chem. Soc.* **1987**, *109*, 3159. Kozik, M.; Casañ-Pastor, N.; Hammer, C. F.; Baker, L. C. W. *J. Am. Chem. Soc.* **1988**, *110*, 1697. Kozik, M.; Baker, L. C. W. *J. Am. Chem. Soc.* **1990**, *112*, 7604. Casañ-Pastor, N.; Baker, L. C. W. *J. Am. Chem. Soc.* **1992**, *114*, 10384.
- (13) Borshch, S. A.; Bigot, B. *Chem. Phys. Lett.* **1993**, *212*, 398.
- (14) Borrás-Almenar, J. J.; Clemente-Juan, J. M.; Coronado, E.; Tsukerblat, B. S. *Chem. Phys.* **1995**, *195*, 1.
- (15) Borrás-Almenar, J. J.; Clemente-Juan, J. M.; Coronado, E.; Tsukerblat, B. S. *Chem. Phys.* **1995**, *195*, 17. Borrás-Almenar, J. J.; Clemente-Juan, J. M.; Coronado, E.; Tsukerblat, B. S. *Chem. Phys.* **1995**, *195*, 29.

- (16) Moreira, I. de P. R.; Illas, F.; Jimenez-Calzado, C.; Fernandez-Sanz, J.; Malrieu, J. P.; Ben Amor, N.; Maynaud, D. *Phys. Rev.* **1999**, *B59*, 6593.
- (17) Durand, P.; Barthelat, J. C. *Theor. Chim. Acta* **1975**, *38*, 283.
- (18) Jimenez-Calzado, C.; Fernandez-Sanz, J.; Malrieu, J. P.; Illas, F. *Chem. Phys. Lett.* **1999**, *307*, 102. Muñoz, D.; Illas, F.; Moreira, I. de P. R. *Phys. Rev. Lett.* **2000**, *84*, 1579. Jimenez-Calzado, C.; Fernandez-Sanz, J.; Malrieu, J. P. *J. Chem. Phys.* **2000**, *112*, 5158.
- (19) Suaud, N.; Lepetit, M.-B. *Phys. Rev.* **2000**, *B62*, 402. Suaud, N.; Lepetit, M.-B. *Phys. Rev. Lett.* **2002**, *88*, 056405.

set and thus cannot hold any bridging pathway between W centers. Therefore, if it is assumed that punctual charges and TIPs mimic properly the electrostatic and Pauli exclusion effects, the role of the PO₄ on the electron delocalization is the difference between the values of the transfer parameters calculated on the PW₄O₂₀ and on the W₄O₁₆ fragments.

The smallest fragments we have considered are formed by the dimeric units W₂O₉ and W₂O₁₀ represented in Figure 1d. In these three cases, the W, O, and P ions that belong to the 4W-based fragments but not to the 2W-based fragments are modeled by punctual charges and TIPs added to the total embedding. The two W₂O₉ fragments, based on corner-sharing pyramids, are extracted from edge-sharing octahedra (rightmost fragment) and corner-sharing octahedra (fragment on the left). The two pyramids of the W₂O₁₀ fragment do not share any atom. These fragments afford the independent evaluation of t' , t , and t^d parameters, respectively. Thus, a comparison with the previous results should permit checking the accuracy of these calculations.

As the structure of the PW₁₂O₄₀ cluster only changes slightly when the charge compensating cations of the salt are changed, all the calculations reported in this work are based on the X-ray crystallographical coordinates⁸ of the (H₅O₂⁺)₃(PW₁₂O₄₀³⁻) salt. In this case, the T_d symmetry of the polyoxometalate makes all the W atoms equivalent. On one hand, this high symmetry permits much quicker calculations. On the other hand, the equivalence of all the W ions induce the equivalence of the interactions W1 ↔ W2 and W3 ↔ W4 (along edge-sharing octahedra) as well as the interactions W1 ↔ W4 and W2 ↔ W3 (along corner-sharing octahedra) and of the interactions W1 ↔ W3 and W2 ↔ W4 between second neighbor octahedra.

III. Model Hamiltonians and Extraction of Parameters

In the reduced Keggin ion, the unpaired electrons are essentially delocalized over the d_{xy} -like orbital of each of the W ions (pointing between the equatorial O ions of the octahedron). Hence, a model Hamiltonian that takes into account the transfer (hopping) parameter between d_{xy} -like orbitals of adjacent W ions and the Coulomb repulsion between the two extra electrons is well suited to reproduce the electron delocalization and spin coupling in this system.¹⁴ We focus in this article on the calculation of the transfer parameters. The extraction of the effective electrostatic repulsions from similar ab initio calculations with a different number of delocalized electrons will be the aim of a forthcoming paper. For an evaluation of these parameters based on pure electrostatic consideration, see ref 14.

A. 4W-Ion Based Fragments. Let us consider one electron delocalized over the 4W-ion based fragments (fragments 1b and c). The model Hamiltonian induces the following doublet states:

$$\Psi_1 = \frac{d_1 + d_2 + d_3 + d_4}{2} \quad (1)$$

$$\Psi_2 = \frac{d_1 - d_2 - d_3 + d_4}{2} \quad (2)$$

$$\Psi_3 = \frac{d_1 + d_2 - d_3 - d_4}{2} \quad (3)$$

$$\Psi_4 = \frac{d_1 - d_2 + d_3 - d_4}{2} \quad (4)$$

where d_1 , d_2 , d_3 , and d_4 stand for the Slater determinants constructed when the extra electron is situated on W1, W2, W3, and W4, respectively.

The transfer parameters are thus written a

$$t = \langle d_1 | H | d_4 \rangle = \langle d_2 | H | d_3 \rangle \quad (5)$$

$$t' = \langle d_1 | H | d_2 \rangle = \langle d_3 | H | d_4 \rangle \quad (6)$$

$$t^d = \langle d_1 | H | d_3 \rangle = \langle d_2 | H | d_4 \rangle \quad (7)$$

The transition energies are

$$E_{1-2} = E_2 - E_1 = -2t' - 2t^d \quad (8)$$

$$E_{1-3} = E_3 - E_1 = -2t - 2t^d \quad (9)$$

$$E_{1-4} = E_4 - E_1 = -2t - 2t' \quad (10)$$

where E_1 , E_2 , E_3 , and E_4 are, respectively, the energies of the states Ψ_1 , Ψ_2 , Ψ_3 , and Ψ_4 ; E_{1-2} , E_{1-3} , and E_{1-4} are, respectively, the transition energies between the states Ψ_1 and Ψ_2 , Ψ_1 and Ψ_3 , and Ψ_1 and Ψ_4 .

The transfer parameters are extracted from the comparison of the transition energies calculated by ab initio methods with eqs 8, 9, and 10.

B. 2W-Ion Based Fragments. Each one of the three 2W-ion based fragments (Figure 1d) supports only one kind of electron transfer. Thus, the fragment on the left is used for extracting t , while the rightmost one allows the evaluation of t' ; finally, from the fragment at the bottom we can extract the value of t^d .

The transition energy E_{DD} between symmetric and antisymmetric doublet states predicted by the model Hamiltonian is thus related to the transfer parameter by the relation:

$$E_{DD} = E_{D+} - E_{D-} = 2t^i$$

where t^i stands for t , t' , or t^d depending on the fragment we are dealing with. E_{D+} and E_{D-} are the energies of the doublet states Ψ_{D+} and Ψ_{D-} , respectively. The symmetry of these two functions are those of $d_1 + d_2$ and $d_1 - d_2$. Thus, for the W₂O₉ fragments, Ψ_{D+} is the antisymmetric doublet and Ψ_{D-} is the symmetric one, whereas, in the W₂O₁₀ fragment, Ψ_{D+} is the symmetric doublet and Ψ_{D-} is the antisymmetric one.

Hence, the energies of the symmetric and antisymmetric doublet states obtained by ab initio calculations directly give the values of the transfer parameters.

IV. Computational Methodology

On each of the previously described fragments, we performed both CASSCF and CASPT2 calculations using the MOLCAS suite of programs.²⁰

According to the physics of mixed-valence compounds that permits the differentiation of the orbitals, depending of their contribution to electron transfer, the CASSCF procedure divides the molecular orbitals into three subspaces: (i) the *inactive orbitals* that remain doubly

(20) Andersson, K.; Barysz, M.; Bernhardsson, A.; Blomberg, M. R. A.; Carissan, Y.; Cooper, D. L.; Cossi, M.; Fleig, T.; Fülscher, M. P.; Gagliardi, L.; de Graaf, C.; Hess, B. A.; Karlström, G.; Lindh, R.; Malmqvist, P.-Å.; Neogrády, P.; Olsen, J.; Roos, B. O.; Schimmelpfennig, B.; Schütz, M.; Seijo, L.; Serrano-Andrés, L.; Siegbahn, P. E. M.; Ståhring, J.; Thorsteinsson, T.; Veryazov, V.; Wierzbowska, M.; Widmark, P.-O. *MOLCAS*, version 5.2; Lund University: Sweden, 2001.

occupied; (ii) the *active orbitals* whose occupation is allowed to change; and (iii) the *virtual orbitals* that remain unoccupied.

The complete active space (CAS) is then defined, for a given number of active electrons (those occupying the active orbitals), as the set of all the Slater determinants that can be built according to the previous occupation rules. The CASSCF consists of the self-consistent optimization of all the orbitals and of the coefficients of the wave function developed on the CAS. It treats exactly the interactions between the active electrons in the mean field of the remaining electrons. That way, the static polarization and a small fraction of the correlation of the active electrons are thus *variationally* taken into account.

From this zeroth order, CASPT2 goes further and takes into account the dynamical polarization and correlation effects in a second-order perturbative treatment; that is as a summation of interactions that do not interact between them. Even if CASPT2 is more precise than CASSCF, we present both results. Indeed, the differences between the two methods account for the influence of the dynamical effects on the transfer parameters, providing at the same time a checking of the suitability of the CASSCF to be a good zeroth order for CASPT2.

Difference dedicated configuration interaction^{21,22} (DDCI) is a more accurate method but often requires much larger calculations than those of CASPT2. In the DDCI method, the dynamical polarization and correlation effects are taken into account variationally; still only those effects that contribute (at the second-order of perturbation) to the energy differences between the states of the CAS are taken into account. This method requires the diagonalization of the matrix representative of the DDCI space generated by all the following excitations on all the determinants of the CAS: (i) 1-hole (one electron is excited from an inactive orbital to an active orbital), (ii) 1-particle (active \rightarrow virtual), (iii) 1-hole-1-particle (inactive \rightarrow virtual), (iv) 2-holes (inactive + inactive \rightarrow active + active), (v) 2-particles (active + active \rightarrow virtual + virtual), (vi) 2-holes-1-particle (inactive + inactive \rightarrow active + virtual), (vii) 1-hole-2-particles (inactive + active \rightarrow virtual + virtual).

Besides the excitations within the DDCI space, other double excitations are also possible, the 2-hole-2-particle excitations which by the way are the most numerous (for a schematic representation of the determinants of the DDCI space and of the 2-hole-2-particle excitations of the CAS, see Figure 2). If we only consider energy differences, these out of space excitations can be ignored when a common set of molecular orbitals (MO) are used for all the calculations.²¹ Indeed in this case, their effect is only to shift the energy of all the states of the CAS by the same energy (at the second-order of perturbation). All the calculations were thus performed on the set of MO optimized at the CASSCF level for the lowest doublet state.

Because of the size of the matrices to diagonalize, the DDCI calculations have only been performed on the 2W-based fragments in order to obtain results as accurate as possible and to compare these results with those obtained with the CASPT2 method. The DDCI results were obtained with the CASDI suite of programs.²³

In our system, the active orbitals are the d_{xy} -like orbital of the W ions. The CAS is thus based on one electron and four orbitals in the case of 4W-based fragment calculations (the corresponding states are those of section 3.1); it is reduced to one electron and two orbitals in the case of 2W-based fragment calculations.

In all the calculations, the inner-core electrons ($[1s^2 2s^2 2p^6 3s^2 3p^6 4s^2 3d^{10} 4p^6 5s^2 4d^{10} 4f^{14}]$ for the W atoms and $[1s^2]$ for the O and P atoms) are represented by effective core potentials (ECP). The outer-core and valence electrons are represented using a 13s10p9d5f primitive basis

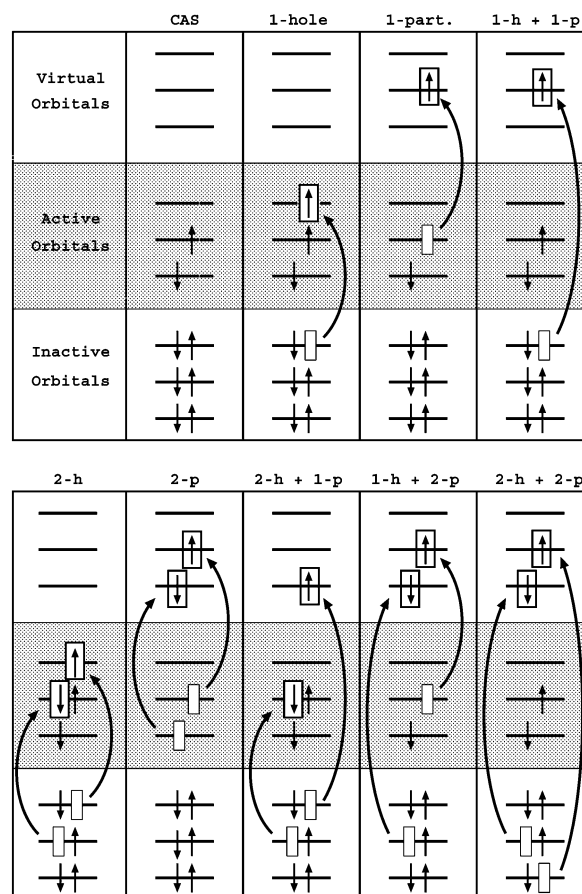


Figure 2. Schematic representation of the single and double excitations on the CAS. The space spanned by {CAS, 1-h, 1-p, 1-h + 1-p, 2-h, 2-p, 2-h + 1-p, 1-h + 2-p} corresponds to the DDCI space. The number of orbitals and electrons in the figure is arbitrary.

Table 1. Results in meV of the Calculations on the 4W-Based Fragments

		PW ₄ O ₂₀	W ₄ O ₁₆
<i>t</i>	CASSCF	-506	-510
	CASPT2	-428	-443
<i>t'</i>	CASSCF	-551	-551
	CASPT2	-470	-479
<i>t^d</i>	CASSCF	-87	-89
	CASPT2	-123	-125

set contracted to 3s3p4d2f for the W, a 5s6p1d primitive basis set contracted to 2s4p1d for the O atoms that belong to the coordination sphere of the W treated in the fragments, a 5s6p1d primitive basis set contracted to 1s2p1d for the other O atoms (the two O the PO₄ molecule not linked to the W of the fragments), and a 7s6p1d primitive basis set contracted to 1s1p1d for the P atom. Exact expressions of the basis sets and ECP can be found in ref 24.

V. Results and Discussion

A. Results on 4W-Ion Fragments. The results obtained on the 4W-ion fragments (fragments b and c in Figure 1) are summarized in Table 1.

As it is generally observed in mixed-valence compounds,^{16,18,19} we can observe that the dynamical effects (the difference between CASPT2 and CASSCF results) remain small and do not change significantly the values of the transfer parameters.

(24) Barandiarán, Z.; Seijo, L. *Can. J. Chem.* **1992**, *70*, 409.

(21) Malrieu, J. P. *J. Chem. Phys.* **1967**, *47*, 4555.

(22) Broer, R.; Maaskant, W. J. A. *J. Chem. Phys.* **1986**, *102*, 103. Miralles, J.; Castell, O.; Caballol, R.; Malrieu, J. P. *J. Chem. Phys.* **1993**, *117*, 33. Cabrero, J.; Ben Amor, N.; de Graaf, C.; Illas, F.; Caballol, R. *J. Phys. Chem.* **2000**, *A104*, 9983.

(23) Maynaud, D.; Ben Amor, N.; Pitarch-Ruiz, J. V. CASDI suite of programs; University of Toulouse: France, 1999. Ben Amor, N.; Maynaud, D.; *Chem. Phys. Lett.* **1998**, *286*, 211. Pitarch-Ruiz, J. V.; Sánchez-Marín, J.; Maynaud, D. *J. Comput. Chem.* **2002**, *23*, 1157.

Table 2. Results in meV of the Calculations on the 2W-Based Fragments

	CASSCF	CASPT2
t	-510	-445
t'	-560	-490
t^d	-80	-102

In contrast with what may be expected, t and t' have very similar values. This is a surprising result, as the W–O–W angles between the two W ions and the bridging oxygen (the oxygen that does not belong to the PO₄ molecule) have very different values. For edge-sharing octahedra, this angle is 127° and for corner-sharing octahedra, it is 153°, whereas the W–O distances have very close values, 1.964 Å and 1.957 Å, respectively. Thus, this angle seems not to be the only relevant parameter involved in the electron transfer. It would be interesting to get a better understanding of all the relevant geometrical parameters that act on the electron-transfer integrals and that can explain why $t \approx t'$. Calculations in this context are presented in the subsection V.C.

The value of t^d is about 4 times smaller with respect to those of t and t' , and of the same sign.

Finally, the very small differences between the results extracted on the PW₄O₂₀ and W₄O₁₆ fragments, less than 15 meV, permit two important conclusions: (i) The bridging effects due to the O anions of the PO₄ molecule are very small, as it could have been expected because of the large distance (≈ 2.5 Å) between these anions and the W atoms. Note that the electron-transfer pathways from one W atom to the other through the PO₄ molecule are allowed in the PW₄O₂₀ fragment but not in the W₄O₁₆ fragment. (ii) The effects of the atoms of the PO₄ molecule on the transfer integrals are accurately reproduced by the chosen charges and TIPs. Whereas in the W₄O₁₆ fragment these atoms are modeled by punctual charges and TIPs, they are treated with a basis set in the PW₄O₂₀ fragment.

These results clearly show the aptness of calculations on a four corner-sharing pyramid embedded fragment, but even for this reduced fragment, the calculations are too large to treat systems where the symmetry between W ions is reduced. Another problem arises from the meaning of the t^d parameter. Indeed, as we extracted three parameters from three energy differences, we could not check the aptness of this parameter to model the system.

We show in the next subsection how calculations on dimer fragments permit the lifting of these two problems.

B. Dimer Calculations. The results of the calculations performed on the three 2W-based fragments are presented in Table 2.

We can see that the results on t and t' compare very well with the results extracted from the W₄O₁₆ fragment with differences smaller than 3% at the CASSCF level as well as at the CASPT2 level. On one hand, this confirms that, as usual in mixed-valence compounds, the electron transfer in the Keggin anion is essentially a local parameter and can be accurately calculated on fragments based on the interacting metal ions and on the atoms of their coordination sphere. On the other hand, these results prove that the effects of the WO₅ pyramids on the atoms of the fragment are correctly reproduced by the chosen punctual charges and TIPs. As the same punctual charges and TIPs were used in the whole embedding, we thus can

assume that the whole embedding correctly reproduces the main effects of the crystal on the fragments¹⁹ (checkings of the aptness of an embedding based on a limited number of punctual charges to reproduce the Madelung field will be presented in a forthcoming paper²⁵ in the case of another polyoxometalate). Hence, the dimer fragment can be considered a quite good model to extract the transfer parameters in a very efficient and simple way.

Concerning t^d , we can see that the values extracted from dimer calculations are significantly different from those extracted from 4W-based fragments, -102 meV versus -125 meV at the CASPT2 level. Indeed, whereas in the two other fragments all the closest neighbors of the bridging O anions are in the fragment, the environment of the bridging O anions in this case is not so accurately treated, since part of the closest neighbors of these anions are modeled by charges and TIPs. Nevertheless, the dimer calculations prove that the t^d parameter has a nonnegligible value and justify our choice to take this parameter into account in the model Hamiltonian. The t^d value obtained from 4W-based fragment is not an artifact because of the extraction of three parameters from three transition energies, and we can trust its value.

Thus, accurate values of electron transfers can be obtained from calculations on correctly embedded small fragments based on only two WO₅ pyramids.

C. Influence of the W–O–W Angle on the Transfer Parameter. We have shown that those O ions shared by the octahedra and the PO₄ molecule do not support any pathway for the electron transfer. Thus, the delocalization only occurs through the orbitals of the other O ions shared by two octahedra. We can wonder if the W–O–W angle formed by the later oxygen and the tungsten ions is the only relevant parameter for the electron transfer, if it can explain why the values of t and t' only differ by about 40–50 meV and if it could be possible to predict the value of these parameters (or at least the ratio between them) only from these crystallographic data.

We have demonstrated that the 2W-based fragments are well designed for extracting the values of t and t' . Thus, we will use these fragments to get more information on the effect of the W–O–W angle on the values of t and t' . For that purpose, we performed calculations on model fragments obtained by rotating each of the WO₅ pyramids around the bridging O atoms in the plane containing these atoms and the two W atoms. 20 model fragments were formed (10 for the transfer between edge-sharing octahedra and 10 for the transfer between corner-sharing octahedra) corresponding to variations of the W–O–W angles of -5°, -4°, -3°, -2°, -1°, +1°, +2°, +3°, +4°, and +5° around the real angles given by the X-ray structure (152.4° for corner-sharing WO₆ octahedra and 126.8° for edge-sharing octahedra). We did not perform calculation on more distorted fragments, as they should be too far from the real structure to give relevant values. The results are represented in Figure 3.

We observe that when the W–O–W angle increases the transfer parameters increase in absolute value. This is due to the increase of the overlap between the magnetic orbital of the W ions and the bridging orbital of the O ion. Such a variation is of the same order of magnitude for corner and edge-sharing

(25) Jimenez-Calzado, C.; Gaita-Ariño, A.; Suaud, N.; Clemente-Juan, J. M.; Coronado, E. To be published.

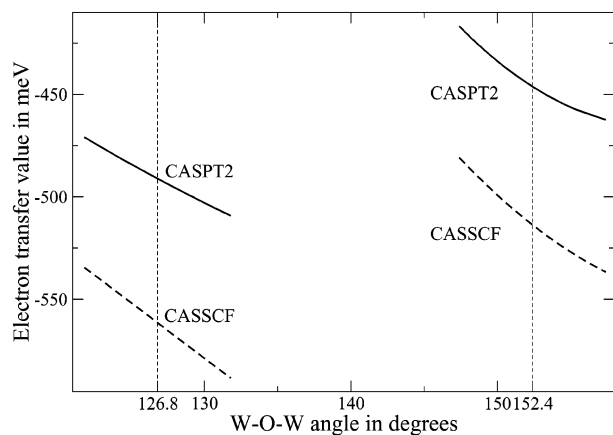


Figure 3. Variations of the value of the electron-transfer parameter with the W–O–W angle around the real structure. The curves on the left represent the variation obtained from edge-sharing fragments; the curves on the right represent the variation obtained from corner-sharing fragments.

fragments with a tangent at 152.4° of about $-4.6 \text{ meV}/^\circ$ and of about $-3.9 \text{ meV}/^\circ$ at 126.8° (at the CASPT2 level).

If the W–O–W angle was the only geometrical parameter acting on the transfer parameter, model fragments based on either corner-sharing octahedra or edge-sharing octahedra should give the same value for the transfer parameter when the W–O–W angle is the same. Extrapolations of the curves presented in Figure 3 clearly show that this is not the case.

Thus, other structural parameters than the W–O–W angle have strong effects on the electron transfer and should be taken into account either to explain why the values of t and t' are close or to roughly predict the values of the electron-transfer parameters in other polyoxometalate clusters.

D. Comparison between CASPT2 and DDCI Results. We have now established the validity of 2W-based fragments, comparing, at the same level of calculations, the values for the transfer parameters extracted from fragments of various nuclearities. It is thus possible on these small fragments to go further than the perturbative treatment of the dynamical effects (CASPT2 method) and perform a variational calculation of the transfer parameters with the DDCI methods. Since the 2W-based fragments calculations give a good evaluation of the order of magnitude of the t^d parameter but with errors of about 20%, it is useless to intend to perform more accurate calculations on such a fragment (and it is at the moment technically impossible to obtain DDCI results on 4W-based fragments). We thus only performed DDCI calculations to evaluate the t and t' parameters, which are the only relevant ones in the theoretical models proposed to describe the magnetic behavior of two-electron-reduced Keggin ions.¹⁴ The results are the following:

$$t = -467 \text{ meV} \quad t' = -507 \text{ meV}$$

These are the most accurate results presented in this work. Differences with the CASPT2 calculations (on the same fragments) are very small, of the order of 20 meV, less than 5%.

Thus, the transfer electron between W atoms of corner-sharing WO_6 octahedra and between W atoms of edge-sharing octahedra have similar intensities, whatever the level of calculation and the fragment used for these calculations.

E. Prediction of the Singlet–Triplet Energy Gap. Theoretical models¹⁴ were previously developed to predict, as a

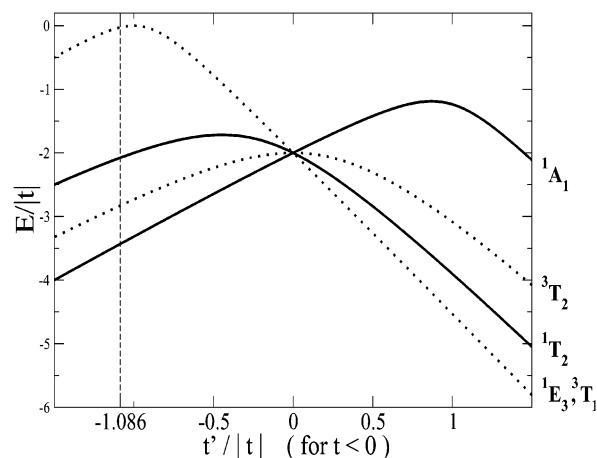


Figure 4. Theoretical energy levels of the doubly reduced Keggin ion. The dotted lines stand for triplet states; the solid lines stand for singlet states (see ref 14 for the denomination of the states). The vertical dashed line represents the value of the calculated $t'/|t|$ ratio.

function of the transfer and electrostatic repulsion parameters, the magnetic behavior of a two-electron-reduced Keggin anion. The symmetry of the Keggin anion exhibits five W–W different distances, $d_I > d_{II} > d_{III} > d_{IV} > d_V$. An evaluation of the V_I , V_{II} , V_{III} , V_{IV} , and V_V corresponding electronic repulsions between the delocalized electrons was performed from purely electrostatic considerations. The differences $V_{III} - V_I \approx 800 \text{ meV}$ and $V_{II} - V_I \approx 300 \text{ meV}$ permitted a first simplification of the model that consists of considering that the electrons remain on centers separated by distances d_I or d_{II} .

The values of the transfer integrals obtained from ab initio calculations give a ratio close to one, $t'/t = 1.086$. They justify the particular case of $t = t'$ and negative that was studied in ref 14. In this case, the energy differences among the three low-lying levels predicted by the model are almost independent of the energy difference $V_{II} - V_I$ in the range $0 < V_{II} - V_I < -10t$. Figure 4 represents the energy levels of the two singlet and two triplet lowest states in the particular case of $V_{II} - V_I = t$. The model predicts a singlet 1A_1 ground state and that the first excited state is a 3T_2 triplet state. The energy gap between these states is thus about $0.6t$, that is 280 meV. This very large value permits an understanding of the diamagnetic properties of two-electron-reduced Keggin anion compounds.¹²

Further improvements of the models allowed by the ab initio evaluation of more parameters would permit a more complete comprehension of the behavior of two-electron-reduced Keggin polyoxoanions and a more accurate prediction of the energy gap between 3T_2 and 1A_1 . This will be the aim of a forthcoming paper.

VI. Conclusion

In this article, we have quantitatively shown for the first time how the electron hopping occurring in mixed-valence Keggin polyoxometalates can promote a strong antiferromagnetic coupling between the pair of delocalized electrons.

To reach this goal, we have combined the exact results obtained from a phenomenological extended Hubbard type model that allows evaluation of the effect of the electron transfer and electron repulsion on the properties of the whole mixed-valence cluster, with ab initio calculations that provide accurate values of the transfer parameters from calculations on small

fragments of the Keggin cluster. These fragments permit large configuration interaction DDCI calculations and, thus, comparison with multireference second-order perturbative theory CASPT2 results, providing at the same time a general and efficient method to extract these parameters in all the polyoxometalate structures.

As a perspective, we want to focus on the computational resources needed for this work. Whereas the calculations on 4W-based fragments were only possible thanks to the power of the center of calculation of the University of Valencia, those performed on dimer fragments (at CASSCF, CASPT2, and DDCI levels) require less than 10Gb of hard disk, 300Mb of memory, and about 30 h on a 866MHz-PIII "home" computer. Our work thus intends to be the grounding of a *low cost general*

study of the transfer parameters in mixed-valence polyoxometalates compounds, and in other kinds of high nuclearity mixed-valence systems.

Acknowledgment. This research was financially supported by European Community (Network Molnanomag, n HPRN-CT-1999-00012), by the spanish Ministerio de Ciencia y Tecnología (MAT2001-3507), and by the Generalitat Valenciana (GV01-312). A.G.-A. thanks the Generalitat Valenciana for a doctoral grant. J.M.C.-J. thanks the spanish Ministerio de Ciencia y Tecnología for a "Ramón y Cajal" contract. We thank Marie-Bernadette Lepetit for many fruitful discussions.

JA027806E